

Fig. 7. Time evolution of the dimensionless radial velocity U for $Ha=60$ and $Gr_{Cr}=6 \times 10^6$ at monitoring point ($R=0.450$, $Z=0.923$). The iso-contours of the dimensionless stream function ψ for various dimensionless times ($\tau_a, \tau_b, \tau_c, \tau_d$) are shown inside the Figure 7.

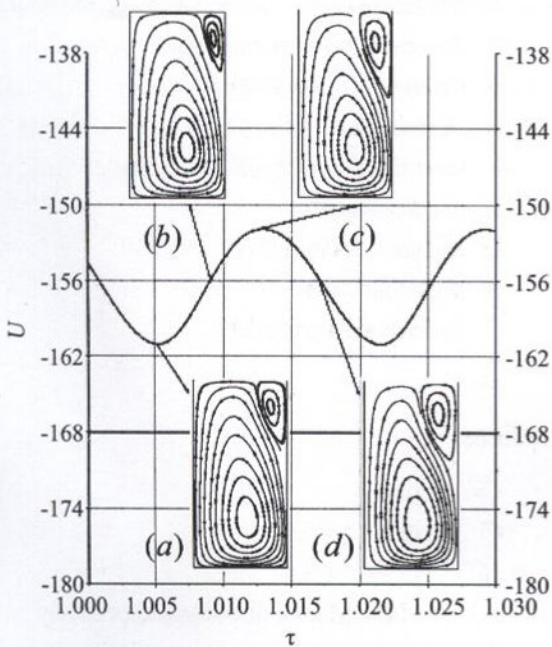


Fig. 8. Time evolution of the dimensionless radial velocity U for $Ha=0$ and $Gr_{Cr}=0.8 \times 10^6$ at monitoring point ($R=0.450$, $Z=0.923$). The iso-contours of the dimensionless stream function ψ for various dimensionless times ($\tau_a, \tau_b, \tau_c, \tau_d$) are shown inside the Figure 8.

character and the oscillatory flow, corresponding to a dominant frequency with its harmonics. Figures 10a and b show the existence of three peaks, however, the value of the first peak $f_{Cr} = 57.91$ for $Ha = 30$ is most dominant, which corresponds to one dominant period for this flow mode $\xi = 1 / f_{Cr}$.

By examining the stability diagram $f_{Cr} - Ha$ (Fig. 11), we can conclude the dependence of the dominant

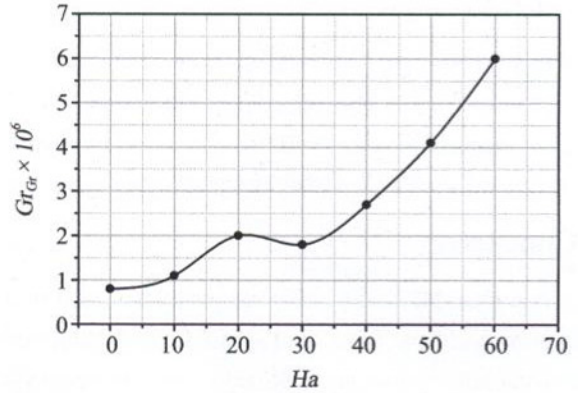


Fig. 9. Stability diagram ($Gr_{Cr} - Ha$).

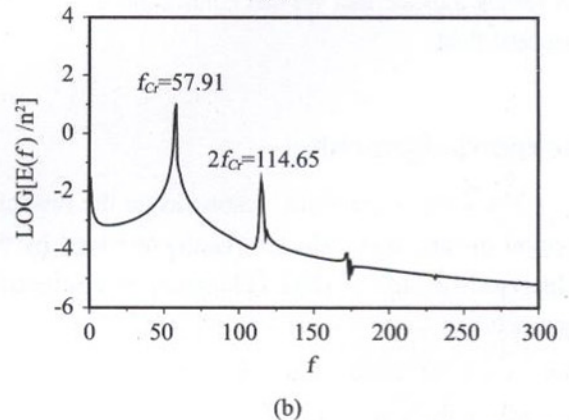
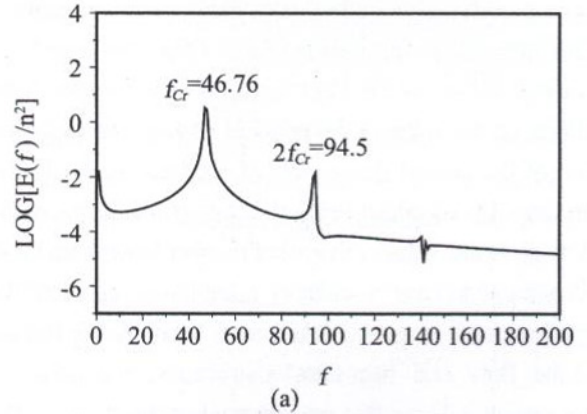


Fig. 10. Power spectrum of the dimensionless radial velocity U : (a) $Ha = 30$ and $Gr_{Cr} = 1.9 \times 10^6$; (b) $Ha = 40$ and $Gr_{Cr} = 2.7 \times 10^6$.